Citation: M. Aranda, G. López-Nicolás, C. Sagüés, M. M. Zavlanos. Distributed formation stabilization using relative position measurements in local coordinates. IEEE Transactions on Automatic Control, vol. 61, no. 12, pp. 3925-3935, 2016.

Distributed Formation Stabilization Using Relative Position Measurements in Local Coordinates

Miguel Aranda, *Member, IEEE*, Gonzalo López-Nicolás, *Senior Member, IEEE*, Carlos Sagüés, *Senior Member, IEEE*, and Michael M. Zavlanos, *Member, IEEE*

***Abstract*—In this paper, we present a novel distributed method to stabilize a set of agents moving in a two dimensional environment to a desired rigid formation. In our approach, each agent computes its control input using the relative positions of a set of formation neighbors but, contrary to most existing works, this information is expressed in the agent's own independent local coordinate frame, without requiring any common reference. The controller is based on the minimization of a Lyapunov function that includes locally computed rotation matrices, which are required due to the absence of a common orientation. Our contribution is that the proposed distributed coordinate-free method achieves global stabilization to a rigid formation with the agents using only partial information of the team, does not require any leader units, and is applicable to both single-integrator or unicycle agents. To guarantee global stability, we require that the network induced by the agent interactions belongs to a certain class of undirected rigid graphs in two dimensions, which we explicitly characterize. The performance of the proposed method is illustrated with numerical simulations.**

***Index Terms*—Distributed control, multi-agent systems, formation stabilization, autonomous mobile robots.**

I. Introduction

Teams of mobile agents capable of autonomous perception, localization, and navigation, can be used to address diverse application scenarios, such as environment surveillance, mapping, exploration, or search and rescue missions, among others. In this paper, we study multiagent formations, which are fundamental to the emergence of many interesting group behaviors. We address, in particular, the problem of distributed formation stabilization [1]. Our goal is to ensure that the positions of a set of mobile agents moving in a two-dimensional space form a desired rigid shape, defined up to translation and rotation.

A formation is often specified by a set of absolute positions attained by the agents in a team [2]–[6]. In this case, controlling the formation requires the use of global positioning sensors (e.g., GPS) on board the agents, or an external localization system. Nevertheless, the availability of such localization systems is often difficult to ensure as, e.g., in the case of agents that operate indoors, where GPS signal is poor. These limitations can be overcome by using relative measurements, as is done in the so-called relative position-based formation stabilization methods [7]–[13]. Still, though, these methods need the agents to have a common sense of orientation. Position-based approaches use linear consensus-based control laws, and ensure global stabilization if the graph that models the interactions between agents (the *formation graph*) is connected. Some of the cited works that use relative measurements assume the common orientation reference is available via sensing, whereas others such as [10], [13] need the agents to agree upon, and subsequently maintain, this required global orientation in a decentralized manner [14].

Relaxing this need for a common sense of orientation is important as it can enhance flexibility of the system by, e.g., permitting operation in GPS-denied environments. Moreover, it can reduce the dependence on complex and expensive sensing and increase the agents' autonomy by enabling them to rely only on low-cost, on-board sensors that do not provide any absolute position or orientation information. In this paper, unlike in all the works cited above, we assume such a *coordinate-free* scenario, where the agents plan their motion relying only on their own independent local coordinates. Similar frameworks that do not require global references have been considered recently in relevant literature on formation stabilization. Next, we review these methods and discuss the differences with our proposed approach. A recent survey of formation controllers focusing on their information requirements and the topology of agent interactions employed can be found in [15].

The method in [16] uses relative pose (i.e., position and orientation) information and considers mobile platforms whose positions and orientations are controlled in a decoupled fashion. Then, for general connected undirected formation graphs, the formation is globally stabilized via two separate consensus-based control laws. In contrast, we assume the agents have single-integrator or unicycle kinematics, and we employ only relative position information. Works that consider relative information commonly specify the formation via interagent distances only, to avoid the difficulty of dealing with inconsistent (i.e., expressed in unaligned frames) position coordinates. This is the approach followed in distance-based formation stabilization methods [17]–[22]. When applied to rigid-shape stabilization problems for arbitrary numbers of agents, these strategies require the formation graph to be rigid [23] and provide only local stability guarantees. Global stabilization to a rigid shape poses significant challenges for these approaches;

Miguel Aranda, Gonzalo López-Nicolás and Carlos Sagüés are with Instituto de Investigación en Ingeniería de Aragón, Universidad de Zaragoza, 50018 Zaragoza, Spain. {marandac, gonlopez, csagues}@unizar.es

Michael M. Zavlanos is with the Dept. of Mechanical Engineering and Materials Science, Duke University, Durham, NC 27708, USA. michael.zavlanos@duke.edu

This work was supported by Ministerio de Economía y Competitividad/European Union (projects DPI2012-32100, DPI2015-69376-R), Ministerio de Educación (FPU grant AP2009-3430), DGA-FSE (group T04), and NSF (CNS # 1261828 and CNS # 1302284).

indeed, as shown in [18], [24], distance-based global formation stabilization is infeasible using gradient descent controllers, which are the most common in the literature. Distance-based schemes require exactly the same information as the method we propose, as knowledge of the directions to the neighboring agents is needed to compute the motion vectors. However, compared to these methods, our approach is globally stable.

Global stabilization to a rigid formation shape using only relative position information expressed in independent local coordinate frames, as in our method, has been achieved by relying on leader agents. Specifically, the distance-based method in [20] achieves global stability for a triangularized graph structure with two leaders. In [25], local relative positions (not just distances) are used in a linear control law based on the complex Laplacian matrix of the formation graph. For a 2-rooted undirected graph, the method globally stabilizes a rigid formation, using two leader agents to fix its scale. Unlike [20], [25], our approach is leaderless. This provides advantages in terms of flexibility and robustness, since it prevents the team's performance from relying heavily on the leaders which, in addition, operate without feedback from the other agents. The work [26] presents a distance-based modified gradient controller where all the agents share a common clock (contrary to our approach) and each adds to its control input an adaptive time-parameterized perturbation. Then, global rigid-shape stabilization is obtained if the formation graph is rigid and no two agents are co-located initially. In the context of formation control, unicycle-type agents are important from a practical perspective [3], [5]–[7], [9], [18], [27]–[30] but introduce additional challenges due to the nonholonomic constraints that restrict their executable motions. To the best of our knowledge, none of the existing distributed, globally convergent, coordinate-free rigid formation controllers [16], [20], [25], [26] considers unicycle-type agents. To the contrary, our method is directly applicable for this kinematics. We also note that some formation control schemes use camera-equipped external units to compute the commands [29]–[31]. In particular, [30] employs multiple partial information-based least-squares image transformations to create the formation. However, as they rely on centralizing external units, this group of methods are neither distributed nor coordinate-free.

The method we propose in this paper stabilizes a group of agents to a rigid shape, using the relative positions of each agent's formation graph neighbors, expressed in local coordinate frames. We capture this control objective by the minimizer of a Lyapunov function that includes this relative position information in full (contrary to distance-based methods), and propose a gradient descent controller that allows us to globally achieve this minimum configuration. Specifically, the proposed Lyapunov function is the sum of cost functions associated with *maximal cliques*, i.e., groups of mutually adjacent agents, in the formation graph. Due to the lack of a shared orientation reference, our Lyapunov function necessarily contains rotation matrices acting on the local relative position vectors, which makes the system dynamics nonlinear. The key idea that enables our approach is to define these rotations as minimizers of the cost functions associated with every maximal clique, and then substitute these expressions in the proposed gradient descent controllers, for which we show that they ensure global stability both for single-integrator and unicycle-type agents. Global stability guarantees require an interaction topology modeled by a class of undirected rigid graphs in two dimensions, which we explicitly characterize. For this class of graphs, in our distributed method each agent computes locally its motion commands, maintains interactions (via sensing or communications) only with its formation graph neighbors, and requires only partial information (specifically, the relative positions of its formation graph neighbors) of the team.

Let us summarize our contribution: to the best of our knowledge, this paper proposes for the first time a method for distributed rigid-shape formation stabilization that uses only locally expressed relative position measurements (i.e., without any common reference), requires each agent to know only partial information of the group, and is globally convergent, leaderless, and applicable for unicycle kinematics. Existing works enjoy a subset of these properties, but not all of them, as discussed in the literature review presented above. Furthermore, an important aspect of our contribution is that we provide a characterization of specific topological conditions for which global stability is ensured. Our related works [32], [33] address coordinate-free formation control and, as we do here, employ rotation matrices computed locally by the agents. However, contrary to the work we present, in both of these prior methods the agents employ global information. [33] uses multi-hop communication that is subject to time delays to propagate the necessary global information to all the agents in the network in a distributed way, while [32] addresses a target enclosing task with agents that move in 3D space.

The contents of the paper are structured as follows. Section II introduces the problem we address and provides necessary background regarding several graph-theoretic concepts. In Section III, we describe the proposed multiagent control strategy, in which the motion commands are locally computed by each of the agents. Section IV presents the stability analysis of our method. We discuss in Section V the class of formation graphs for which the controller is ensured to be stable. Section VI describes results from simulations carried out to evaluate our approach. Finally, the conclusion of the paper and directions for future work are presented in Section VII.

II. Problem formulation and background

Consider a group of N mobile agents in $\mathbb{R}^2$. Let us denote, in an arbitrary global reference frame, the position of agent i, $i = 1, ..., N$, as $\mathbf{q_i} = [q_i^x, q_i^y]^T \in \mathbb{R}^2$ and its orientation as $\phi_i \in \mathbb{R}$. We assume each agent i obeys unicycle kinematics, as follows:

$$\dot{q}_i^x = -v_i \sin\phi_i, \;\; \dot{q}_i^y = v_i \cos\phi_i, \;\; \dot{\phi}_i = -\omega_i, \tag{1}$$

where $v_i \in \mathbb{R}$ is its linear velocity input and $\omega_i \in \mathbb{R}$ is its angular velocity input. We will additionally consider the single-integrator model, where the orientation of each agent is not relevant and its dynamics is determined by a velocity input $\mathbf{u_i} \in \mathbb{R}^2$:

$$\dot{\mathbf{q}}_\mathbf{i} = \mathbf{u_i}. \tag{2}$$

We define a desired configuration, or formation shape, by a certain, fixed, reference layout of the positions of the N agents in their configuration space. The way in which we encode the desired configuration is through a set of interagent relative position vectors. To model the interactions between agents, we define a static undirected formation graph $\mathcal{G}_f = (\mathcal{V}, \mathcal{E})$, as is typical in related work on formation control, e.g., [20], [25], [26]. Each node in $\mathcal{V}$ is associated with an agent, and we assume that each agent can obtain, using its sensing or communication capabilities, an estimate of the relative positions of its fixed set of neighbors in $\mathcal{G}_f$.

Then, for every neighbor j of agent i, we denote as $\mathbf{c_{ji}} \in \mathbb{R}^2$ the vector from i to j in the reference layout of the agents that defines the desired configuration. The agents are not interchangeable, i.e., each of them has a fixed place in the target formation. We then consider that the N agents are in the desired configuration if the reference layout has been achieved, up to an arbitrary rotation and translation, i.e., if it holds that:

$$\mathbf{q_{ji}} = \mathbf{R}\mathbf{c_{ji}}, \ \ \forall i, j = 1, ..., N, \tag{3}$$

where we define $\mathbf{q_{ji}} = \mathbf{q_j} - \mathbf{q_i}$, and $\mathbf{R} \in SO(2)$ is an arbitrary rotation matrix. Thus, the problem that we set out to solve in this paper is specified as follows:

Problem 1. *Given an initial configuration in which the agents are in arbitrary positions, find a control strategy that stabilizes them in a set of final positions such that the group is in the desired configuration.*

A. Graph theory

Next, we discuss a series of definitions relevant to undirected graphs that are used throughout the paper. A *clique* in a graph $\mathcal{G}$ is a complete subgraph, i.e., a subset of its nodes and edges such that every two nodes are adjacent. An *n-node clique* is a clique containing n nodes. A *maximal clique* is one that cannot be augmented by incorporating one more node. The intersection of two cliques is given by the sets of nodes and edges they share. The *p-clique graph*, with $p \geq 1$, of $\mathcal{G}$, denoted as $\mathcal{C}_p(\mathcal{G})$, is a graph whose nodes are the maximal cliques of $\mathcal{G}$, and where two nodes are adjacent if the intersection of their associated cliques contains at least p nodes [34]. A graph is called a tree if any two of its nodes are connected by exactly one sequence of edges. A leaf in a tree graph is a node of degree one. An induced subgraph of $\mathcal{G}$ is a graph that includes a subset of its nodes and all those edges of $\mathcal{G}$ that join two nodes in the subset.

III. Control strategy

Let us assume there are M maximal cliques in $\mathcal{G}_f$. For $m = 1, ..., M$, we denote as I_m the set of indices of the nodes that form the $m-th$ clique, and $N_m = card(I_m)$. We interchangeably refer in the paper to the nodes of $\mathcal{G}_f$ as nodes or agents. We define, in an arbitrary global coordinate frame, the following cost function for each maximal clique:

$$\gamma_m = \frac{1}{2N_m} \sum_{j \in I_m} || \sum_{k \in I_m} \mathbf{q_{jk}} - \mathbf{R_m}\mathbf{c_{jk}}||^2, \tag{4}$$

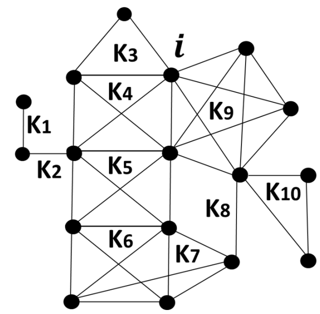

Fig. 1. An arbitrary formation graph $\mathcal{G}_f$ with $N = 17$ nodes and $M = 10$ maximal cliques, denoted as K_m, $m = 1, ..., M$. The size of the maximal cliques ranges from two to five nodes. For instance, K_1 contains two agents, K_3 contains three agents, K_4 contains four, and K_9 consists of five agents. Trivial single-node maximal cliques, which would represent isolated nodes of $\mathcal{G}_f$, are not contemplated. Our formation controller is based on the minimization of a global cost function γ that is the aggregate of partial functions γ_m associated with the maximal cliques. Each agent operates on the set of maximal cliques it belongs to, e.g., the motion of agent i pursues the minimization of the sum of γ_3, γ_4, and γ_9, for which it uses the knowledge of the locally expressed relative positions of its neighbors in $\mathcal{G}_f$. To ensure stabilization to a rigid formation, $\mathcal{G}_f$ must satisfy certain rigidity-related conditions, as explained throughout the paper.

where $\mathbf{R_m} \in SO(2)$ is a rotation matrix whose value, equal for all the agents in the clique, is discussed in the following section. Note that, for simplicity of the notation, we include in (4) the null terms occurring when $j = k$. Now, observe that if $\gamma_m = 0$, we can write, considering in (4) the addends associated with two given agents $j = i_1$ and $j = i_2$:

$$\sum_{k \in I_m} \mathbf{q_{i_1 k}} - \mathbf{R_m}\mathbf{c_{i_1 k}} = 0, \ \sum_{k \in I_m} \mathbf{q_{i_2 k}} - \mathbf{R_m}\mathbf{c_{i_2 k}} = 0. \tag{5}$$

Subtracting the two equations, we have that $\mathbf{q_{i_1 i_2}} = \mathbf{R_m}\mathbf{c_{i_1 i_2}}$, which holds for every pair i_1, i_2 in I_m. Hence, if $\gamma_m = 0$, the subset of agents in the $m-th$ clique are in the desired configuration with one another (we will refer to this as a sub-formation). We can then see that γ_m encodes how distant the agents are from reaching the $m-th$ sub-formation. We define the global cost function for our system as follows:

$$\gamma = \sum_{m=1,...,M} \gamma_m, \tag{6}$$

so that if γ vanishes, all the sub-formations are attained. Note that every node and every edge of $\mathcal{G}_f$ are part of one or multiple maximal cliques. Thus, if $\{i, j\} \in \mathcal{E}$, the relative vectors between i and j contribute to at least one γ_m (4). This means that, by encompassing all the M maximal cliques, the global function γ captures all the edges in $\mathcal{G}_f$. An illustration of the structure of maximal cliques that is the basis of our controller is provided in Fig. 1.

A. Rotation matrices

We set out to drive γ to zero, which implies doing so for every γ_m. Accordingly, the rotation matrix in each function γ_m (4) is chosen so as to minimize it, as shown next. Let us note that the analysis in this section is analogous to finding the solution to the orthogonal Procrustes problem [35].

We define $\mathbf{R_m}$ as a rotation by an angle α_m, i.e.,:

$$\mathbf{R_m} = \begin{bmatrix} \cos\alpha_m & -\sin\alpha_m \\ \sin\alpha_m & \cos\alpha_m \end{bmatrix}. \quad (7)$$

Let us express γ_m in terms of α_m and the components of the relative position vectors, $\mathbf{q_{jk}} = [q^x_{jk}, q^y_{jk}]^T$, $\mathbf{c_{jk}} = [c^x_{jk}, c^y_{jk}]^T$:

$$\gamma_m = \frac{1}{2N_m} \sum_{j\in I_m} \Big[(\sum_{k\in I_m} q^x_{jk} - c^x_{jk}\cos\alpha_m + c^y_{jk}\sin\alpha_m)^2 \quad (8)$$
$$+ (\sum_{k\in I_m} q^y_{jk} - c^x_{jk}\sin\alpha_m - c^y_{jk}\cos\alpha_m)^2 \Big].$$

Let us introduce the notation: $\mathbf{S_{qj}} = [S^x_{qj}, S^y_{qj}]^T = \sum_{k\in I_m} \mathbf{q_{jk}}$ and $\mathbf{S_{cj}} = [S^x_{cj}, S^y_{cj}]^T = \sum_{k\in I_m} \mathbf{c_{jk}}$. To minimize γ_m with respect to α_m, we solve $\frac{\partial\gamma_m}{\partial\alpha_m} = 0$. After manipulation, this derivative is:

$$\frac{\partial\gamma_m}{\partial\alpha_m} = \frac{1}{N_m} \Big[\sin\alpha_m \sum_{j\in I_m} (S^x_{qj}S^x_{cj} + S^y_{qj}S^y_{cj})$$
$$- \cos\alpha_m \sum_{j\in I_m} (-S^x_{qj}S^y_{cj} + S^y_{qj}S^x_{cj}) \Big]. \quad (9)$$

Then, the condition $\frac{\partial\gamma_m}{\partial\alpha_m} = 0$ is expressed as:

$$\sin\alpha_m \sum_{j\in I_m} \mathbf{S^T_{qj}S_{cj}} - \cos\alpha_m \sum_{j\in I_m} \mathbf{S^T_{qj}S^\perp_{cj}} = 0, \quad (10)$$

where the superscript $\perp$ denotes a rotation of a vector by $\pi/2$ radians, as follows: $\mathbf{S^\perp_{cj}} = [(0,1)^T, (-1,0)^T]\mathbf{S_{cj}}$. Solving (10) with respect to the rotation angle α_m, we get:

$$\alpha_m = \arctan \frac{\sum_{j\in I_m} \mathbf{S^T_{qj}S^\perp_{cj}}}{\sum_{j\in I_m} \mathbf{S^T_{qj}S_{cj}}}. \quad (11)$$

Observe from (11) that there are two possible solutions for α_m, separated by π radians. In order to select the correct one, we compute the second order derivative from (9):

$$\frac{\partial^2\gamma_m}{\partial\alpha_m^2} = \frac{1}{N_m} \Big[\cos\alpha_m \sum_{j\in I_m} \mathbf{S^T_{qj}S_{cj}} + \sin\alpha_m \sum_{j\in I_m} \mathbf{S^T_{qj}S^\perp_{cj}} \Big]. \quad (12)$$

By considering together (10) and (12), it can be readily seen that one of the solutions for (11) minimizes γ_m, while the other maximizes the function. The solution that is a minimum satisfies the condition $\frac{\partial^2\gamma_m}{\partial\alpha_m^2} > 0$. If we isolate the term $\cos\alpha_m$ in (10) and then substitute it in (12), we easily get that this condition holds when $\sin(\alpha_m)/\sum_{j\in I_m} \mathbf{S^T_{qj}S^\perp_{cj}} > 0$, i.e., $\sin(\alpha_m)$ must have the same sign as the numerator in the $\arctan$ function in (11). This implies that, among the two possible values of α_m, the one that minimizes γ_m, i.e., the value used in our controller, is given by:

$$\alpha_m = atan2(\sum_{j\in I_m} \mathbf{S^T_{qj}S^\perp_{cj}}, \sum_{j\in I_m} \mathbf{S^T_{qj}S_{cj}}), \quad (13)$$

where the $atan2$ function returns the solution of (11) for which α_m is in the quadrant that corresponds to the signs of the two input arguments. Note that the case $atan2(0,0)$, for which α_m is not defined, is theoretically possible in (13) for degenerate configurations of the agents' positions where γ_m is constant for all α_m, see (10). In general terms, the singular or degenerate cases are linked to the desired geometry and not to our control strategy. Multiple agents occupying the same position is another particular example of a degenerate arrangement. All these possible configurations are measure zero, i.e., they will never occur in practice and, therefore, we do not consider them in our analysis.

B. Control law

Our controller is based on each agent i following the negative gradient of the cost function γ with respect to $\mathbf{q_i}$. Let us look at one given clique, m, that contains agent i. We have:

$$\nabla_{\mathbf{q_i}}\gamma_m = \frac{\partial\gamma_m}{\partial\alpha_m}\frac{\partial\alpha_m}{\partial\mathbf{q_i}} + \frac{\partial\gamma_m}{\partial\mathbf{q_i}} = \frac{\partial\gamma_m}{\partial\mathbf{q_i}}, \quad (14)$$

given that, as discussed in Section III-A, $\frac{\partial\gamma_m}{\partial\alpha_m} = 0$. Thus, we focus next on the partial differentiation with respect to $\mathbf{q_i}$. For clarity of the exposition, let us express γ_m (4) as a sum of components:

$$\gamma_m = \sum_{j\in I_m} \gamma_{m_j}, \quad \gamma_{m_j} = \frac{1}{2N_m} || \sum_{k\in I_m} \mathbf{q_{jk}} - \mathbf{R_m c_{jk}} ||^2. \quad (15)$$

For the component corresponding to $j = i$, we have:

$$\frac{\partial\gamma_{m_j}}{\partial\mathbf{q_i}} = \frac{\partial\gamma_{m_i}}{\partial\mathbf{q_i}} = \frac{1}{N_m} \sum_{k\in I_m} (\mathbf{q_i} - \mathbf{q_k} - \mathbf{R_m c_{ik}})(N_m - 1)$$
$$= (1 - \frac{1}{N_m}) \sum_{k\in I_m} (\mathbf{q_{ik}} - \mathbf{R_m c_{ik}}), \quad (16)$$

whereas each of the components in (15) such that $j \neq i$ gives:

$$\frac{\partial\gamma_{m_j}}{\partial\mathbf{q_i}} = \frac{1}{N_m} \sum_{k\in I_m} (\mathbf{q_j} - \mathbf{q_k} - \mathbf{R_m c_{jk}})(-1)$$
$$= \frac{-1}{N_m} \sum_{k\in I_m} (\mathbf{q_{jk}} - \mathbf{R_m c_{jk}}). \quad (17)$$

From (15), and substituting and grouping (16) and (17), we get:

$$\frac{\partial\gamma_m}{\partial\mathbf{q_i}} = \frac{\partial\gamma_{m_i}}{\partial\mathbf{q_i}} + \sum_{\substack{j\in I_m \\ j\neq i}} \frac{\partial\gamma_{m_j}}{\partial\mathbf{q_i}}$$
$$= \sum_{k\in I_m} (\mathbf{q_{ik}} - \mathbf{R_m c_{ik}}) - \frac{1}{N_m} \sum_{j\in I_m} \sum_{k\in I_m} (\mathbf{q_{jk}} - \mathbf{R_m c_{jk}}). \quad (18)$$

Observe now that:

$$\sum_{j\in I_m} \sum_{k\in I_m} \mathbf{q_{jk}} = N_m(\sum_{j\in I_m} \mathbf{q_j} - \sum_{k\in I_m} \mathbf{q_k}) = \sum_{j\in I_m} \sum_{k\in I_m} \mathbf{c_{jk}} = \mathbf{0}. \quad (19)$$

Substituting (19) in (18) and then renaming the index k as j, for convenience, we finally get:

$$\frac{\partial\gamma_m}{\partial\mathbf{q_i}} = \sum_{j\in I_m} \mathbf{q_{ij}} - \mathbf{R_m c_{ij}}. \quad (20)$$

Let us denote, for every agent i, the set of maximal cliques to which it belongs as C_i, $i = 1, ..., N$. Note that, clearly,

$\frac{\partial \gamma_m}{\partial \mathbf{q_i}} = \mathbf{0}$ if m is not in C_i. We can now differentiate the global cost function (6). Substituting (14) and (20), we have:

$$\nabla_{\mathbf{q_i}} \gamma = \sum_{m=1,\ldots,M} \nabla_{\mathbf{q_i}} \gamma_m$$
$$= \sum_{m=1,\ldots,M} \frac{\partial \gamma_m}{\partial \mathbf{q_i}} = \sum_{m \in C_i} \left[\sum_{j \in I_m} \mathbf{q_{ij}} - \mathbf{R_m} \mathbf{c_{ij}} \right]. \quad (21)$$

Let us define the *partial* desired motion vector for agent i due to clique m as:

$$\mathbf{d_{i_m}} = \sum_{j \in I_m} \mathbf{q_{ji}} - \mathbf{R_m} \mathbf{c_{ji}}. \quad (22)$$

Negating the gradient in (21), we obtain what we will call the desired motion vector for agent i, $\mathbf{d_i}$, which equals the sum of partial desired motion vectors $\mathbf{d_{i_m}}$ over the cliques in C_i:

$$\mathbf{d_i} = -\nabla_{\mathbf{q_i}} \gamma = \sum_{m \in C_i} \left[\sum_{j \in I_m} \mathbf{q_{ji}} - \mathbf{R_m} \mathbf{c_{ji}} \right] = \sum_{m \in C_i} \mathbf{d_{i_m}}. \quad (23)$$

Considering single-integrator kinematics, we propose to define each agent's control input directly as:

$$\mathbf{u_i} = \dot{\mathbf{q}}_\mathbf{i} = k_c \mathbf{d_i}, \quad (24)$$

where $k_c > 0$ is a control gain. If, instead, the agents have unicycle kinematics, we define β_i as the angular alignment error, measured in the interval $(-\pi, \pi]$, between agent $i's$ current heading and the direction of its desired motion vector (see Fig. 2, left). If $\mathbf{d_i} = \mathbf{0}$, we define $\beta_i = 0$. Then, we propose the following control law:

$$\begin{cases} v_i = \begin{cases} k_v ||\mathbf{d_i}||, & \text{if} \quad |\beta_i| < \frac{\pi}{2} \\ 0, & \text{if} \quad |\beta_i| \geq \frac{\pi}{2} \end{cases} \\ \omega_i = k_\omega \beta_i, \end{cases} \quad (25)$$

where $k_v > 0$ and $k_\omega > 0$ are control gains. Observe that when $|\beta_i| \geq \frac{\pi}{2}$, the agent only rotates in place and does not translate.

C. Information requirements

Let us specify the information that a given agent needs so as to compute its control input.

Note that the control laws above define a distributed system which relies on the use of only partial information of the multiagent team. For each agent i, its control input is obtained using only the knowledge of $\mathbf{d_i}$, which is obtained, (23), (13), from the relative position vectors corresponding to the agents belonging to the cliques in C_i, i.e., the agents which are neighbors of i in $\mathcal{G}_f$. That is, defining $\mathcal{N}_i$ as $i's$ set of formation graph neighbors, agent i needs to know the measurements $\mathbf{q_{ji}}$, $\forall j \in \mathcal{N}_i$. In particular, note that i can directly compute, by itself, the rotation angles α_m (13) for $m \in C_i$ by using these measurements. It is clear that agent i also has to know the labels, or identifications, of its neighboring agents. In addition, it needs the local structure of the formation graph, i.e., which agents form each of the maximal cliques i belongs to. In our notation: I_m for $m \in C_i$.

Finally, note that agent i only needs to know the above quantities expressed in its own independent *local coordinates*, as explained in the next section.

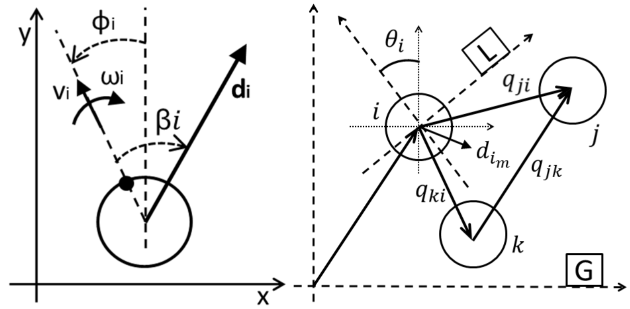

Fig. 2. Left: Depiction of the variables used in our controller for an agent i with unicycle kinematics. Right: Representation of the quantities used to compute $i's$ control law, expressed in an arbitrary global frame G. Three agents i, j and k in a maximal clique m are depicted, and the local frame L of i is shown.

D. Computation of the control inputs in the local frames

A central property of the method we propose is that each agent can compute its control input in the absence of a global orientation reference, as shown next. We denote as θ_i the rotation angle between the arbitrary global frame and the local frame in which agent i operates, and by $\mathbf{P_i}(\theta_i) \in SO(2)$ the corresponding rotation matrix. Let us now write down the partial desired motion vector for clique m (the analysis can be trivially extended to the desired motion vectors $\mathbf{d_i}$) computed locally by i (22), using a superscript Li to denote that the quantities are expressed in $i's$ local frame:

$$\mathbf{d_{i_m}^{Li}} = \sum_{j \in I_m} \mathbf{q_{ji}^{Li}} - \mathbf{R_m^{Li}} \mathbf{c_{ji}}. \quad (26)$$

Let us show how the rotation matrices computed in the global and local frames are related. We recall (4), which expresses γ_m in an arbitrary global frame:

$$\gamma_m = \frac{1}{2N_m} \sum_{j \in I_m} || \sum_{k \in I_m} \mathbf{q_{jk}} - \mathbf{R_m} \mathbf{c_{jk}} ||^2. \quad (27)$$

Agent i minimizes the cost function expressed in its local frame, i.e., γ_m^{Li}. Given that $\mathbf{q_{jk}^{Li}} = \mathbf{P_i} \mathbf{q_{jk}}$ for all $j, k \in I_m$, we can write, using simple manipulation:

$$\gamma_m^{Li} = \frac{1}{2N_m} \sum_{j \in I_m} || \sum_{k \in I_m} \mathbf{q_{jk}^{Li}} - \mathbf{R_m^{Li}} \mathbf{c_{jk}} ||^2 =$$
$$\frac{1}{2N_m} \sum_{j \in I_m} || \sum_{k \in I_m} \mathbf{q_{jk}} - \mathbf{P_i^{-1}} \mathbf{R_m^{Li}} \mathbf{c_{jk}} ||^2. \quad (28)$$

Given that $\mathbf{R_m}$ minimizes γ_m and $\mathbf{R_m^{Li}}$ minimizes γ_m^{Li}, and this minimum is unique (Section III-A), we clearly have from (27) and (28) that $\gamma_m = \gamma_m^{Li}$ and hence $\mathbf{R_m} = \mathbf{P_i^{-1}} \mathbf{R_m^{Li}}$, i.e., $\mathbf{R_m^{Li}} = \mathbf{P_i} \mathbf{R_m}$. Thus, from (26):

$$\mathbf{d_{i_m}^{Li}} = \sum_{j \in I_m} \mathbf{q_{ji}^{Li}} - \mathbf{R_m^{Li}} \mathbf{c_{ji}} = \sum_{j \in I_m} \mathbf{P_i} \mathbf{q_{ji}} - \mathbf{P_i} \mathbf{R_m} \mathbf{c_{ji}} = \mathbf{P_i} \mathbf{d_{i_m}}, \quad (29)$$

which means that the computations referred to the two frames give an identical desired motion vector. Figure 2 (right) illustrates the variables used by the controller with respect to the global and local frames.

IV. Stability analysis

In this section, we study the stability of the proposed control strategy. Throughout the section, we assume $\mathcal{G}_f$ to be a static graph. Note that, unless otherwise stated, all the entities in the Euclidean plane are expressed in an arbitrary global reference frame. Our control methodology, described in the previous section, is based on minimizing a cost function (6) defined over the set of maximal cliques in the formation graph. We present a stability analysis that relies on a description of this graph in terms of its maximal-clique intersection sets. Specifically, we use 2-clique graphs to capture these intersections. Let us denote the 2-clique graph of $\mathcal{G}_f$ as $\mathcal{C}_2(\mathcal{G}_f) = (\mathcal{V}_{\mathcal{C}_2}, \mathcal{E}_{\mathcal{C}_2})$. We will refer equivalently to the maximal cliques of $\mathcal{G}_f$ or to the nodes of $\mathcal{C}_2(\mathcal{G}_f)$. Consider the following assumption:

A1) $\mathcal{C}_2(\mathcal{G}_f)$ is connected.

Observe that this assumption immediately implies that there cannot be maximal cliques of size one or two in $\mathcal{G}_f$. Therefore, every agent is in at least one 3-node clique of $\mathcal{G}_f$. Figure 3 shows an example $\mathcal{G}_f$ for which A1 is satisfied, and its 2-clique graph.

Theorem 1. *If A1 holds, the multiagent system under the control laws (24), for single-integrator kinematics, or (25), for unicycle kinematics, is locally stable with respect to the desired configuration.*

Proof. We will use Lyapunov analysis to prove the stability of the system. Let us define a Lyapunov candidate function as $V = \gamma$. It is straightforward to see that V is positive semi-definite and radially unbounded. In addition, the equilibrium $V = 0$ occurs if and only if the N agents are in the desired configuration, as shown next.

Let us assume the agents are in the desired configuration and see that this leads to $V = 0$. Observe that this situation implies that for every pair i, j in $1, ..., N$, $\mathbf{q_{ij}} = \mathbf{R}\mathbf{c_{ij}}$, where $\mathbf{R}$ expresses the rotation of the formation pattern (3). Since this holds for every pair of agents, notice in (4) that γ_m is zero, i.e., has its minimum possible value, $\forall m = 1, ..., M$, if $\mathbf{R_m} = \mathbf{R}$. Clearly, since every $\mathbf{R_m}$ must be such that its associated γ_m is minimum (Section III-A), we have that all of the rotations are equal to $\mathbf{R}$. Thus, $V = \gamma = 0$.

On the other hand, assume $V = 0$, which implies, since $\gamma_m = 0 \; \forall m = 1, ..., M$, that all the sub-formations for each of the M maximal cliques have been achieved (Section III). Note, however, that this does not imply, in general, that the agents are in the global desired formation. To guarantee this, we use assumption A1 next. Note that the assumption implies that the agents form a structure of maximal cliques which have, at least, three nodes each, and for every maximal clique m_1, there exists at least one other maximal clique m_2 such that m_1 and m_2 have at least two agents in common. Then, consider two given agents i, j which are in the intersection of two given cliques m_1 and m_2. It is clear, since $\gamma = 0$, that $\mathbf{q_{ij}} = \mathbf{R_{m_1}}\mathbf{c_{ij}} = \mathbf{R_{m_2}}\mathbf{c_{ij}}$ and, therefore, $\mathbf{R_{m_1}} = \mathbf{R_{m_2}}$. Now, due to connectedness of $\mathcal{C}_2(\mathcal{G}_f)$, this equality can be trivially propagated throughout the M maximal cliques. Thus, $\mathbf{R_m} = \mathbf{R} \; \forall m = 1, ..., M$, which means that $\mathbf{q_{ij}} = \mathbf{R}\mathbf{c_{ij}} \; \forall i, j = 1, ..., N$, i.e., the N agents are in the desired configuration. After showing that $V = 0$ provides a characterization of the desired formation, we study next the stability of the system by analyzing the dynamics of V. Notice that, given the negative gradient-based control strategy expressed in (23), we can write:

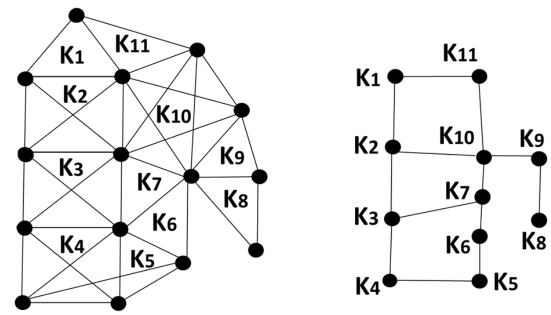

Fig. 3. Illustration of 2-clique graphs, which are used in the topological characterizations provided in the paper. Left: a given formation graph $\mathcal{G}_f$, with maximal cliques K_m, $m = 1, ..., 11$. Right: the 2-clique graph of $\mathcal{G}_f$, $\mathcal{C}_2(\mathcal{G}_f)$, which is connected (i.e., the topology satisfies assumption A1.)

$$\dot{V} = \sum_{i=1,...,N} (\nabla_{\mathbf{q_i}} V)^T \dot{\mathbf{q}}_\mathbf{i} = - \sum_{i=1,...,N} \mathbf{d_i^T} \dot{\mathbf{q}}_\mathbf{i}. \quad (30)$$

Then, considering our controller for single-integrator kinematics (24), we have, by direct substitution:

$$\dot{V} = -k_c \sum_{i=1,...,N} ||\mathbf{d_i}||^2 \leq 0. \quad (31)$$

Let us now consider unicycle kinematics. We denote as S_v the time-varying set of agents for which it holds that $|\beta_i| < \pi/2$. Since the displacement of a unicycle agent always occurs along the direction of its current heading, we have in our case that, from the linear velocity in (25), the motion vector executed by each agent i (see Fig. 2) is:

$$\dot{\mathbf{q}}_\mathbf{i} = \begin{cases} k_v \mathbf{Q}(\beta_i) \mathbf{d_i}, & i \in S_v \\ \mathbf{0}, & i \notin S_v, \end{cases} \quad (32)$$

where $\mathbf{Q}(\beta_i) \in SO(2)$ expresses a rotation by the angular alignment error. Then, substituting (32) in (30):

$$\dot{V} = -k_v \sum_{i \in Sv} \cos(\beta_i) ||\mathbf{d_i}||^2 + \sum_{i \notin Sv} (0) \leq 0, \quad (33)$$

where the condition that $\dot{V}$ can never be positive results from the fact that $|\beta_i| < \pi/2 \; \forall i \in S_v$, i.e., $\cos(\beta_i) > 0 \; \forall i \in S_v$. By virtue of the global invariant set theorem, (31) and (33) ensure that, under the proposed control laws for single-integrator (24) or unicycle (25) kinematics, the system converges asymptotically to the largest invariant set in the set $W = \{\mathbf{q_i}, i = 1, ..., N \mid \dot{V} = 0\}$. Therefore, it can be concluded that the multiagent system is locally stable with respect to the desired formation (i.e., $V = 0$). ☐

Corollary 1. *If A1 is satisfied, then all stable equilibriums of the multiagent system under the controllers for single-integrator (24) or unicycle (25) kinematics are static configurations, and occur if and only if* $\mathbf{d_i} = \mathbf{0} \; \forall i = 1, ..., N$.

Proof. By a stable equilibrium we precisely mean a configuration that the system will not get out of, i.e., a configuration for which it holds that $\dot{V} = 0$ for all time. Let us examine these equilibriums. We look at the controller for single-integrator agents first. We immediately see from (31) that $\dot{V} = 0 \Leftrightarrow \mathbf{d_i} = \mathbf{0}\, \forall i = 1, ..., N$. If all $\mathbf{d_i}$ are null, all the agents are static, see (24). This also clearly implies the equilibrium is stable. Thus, the statement of the Corollary holds. For unicycle kinematics, suppose $\dot{V} = 0$ at some instant. Notice from (33) that this implies $\mathbf{d_i} = \mathbf{0}\, \forall i \in S_v$. These agents are static (25). However, it is possible that for some of the agents not belonging to S_v, $\mathbf{d_i} \neq \mathbf{0}$. Assume this is the case. Note that even if their desired vectors are not null, the agents not in S_v can never translate, due to the linear velocity defined in (25). As a result, we have that $\dot{V} = 0$ implies that none of the N agents' positions, $\mathbf{q_i}$, can change. Therefore, from (23), no $\mathbf{d_i}$ can change. The vectors $\mathbf{d_i}$ being constant implies that every agent not belonging to S_v such that its $\mathbf{d_i} \neq \mathbf{0}$ will rotate in place, thanks to the angular velocity control in (25), seeking to align itself with the direction of its constant $\mathbf{d_i}$. This will eventually lead, at some time instant, to $|\beta_i| < \pi/2$ for one of these agents, i.e., $\cos(\beta_i) > 0$ and, given that $\mathbf{d_i} \neq \mathbf{0}$, to $\dot{V} < 0$ (33), i.e., the assumed equilibrium is not stable. Hence, we can conclude that if the system is in a stable equilibrium, i.e., $\dot{V} = 0$ for all time, it must hold that $\mathbf{d_i} = \mathbf{0}\ \forall i = 1, ..., N$. The converse statement $\mathbf{d_i} = \mathbf{0}\ \forall i = 1, ..., N \Rightarrow \dot{V} = 0$ for all time is immediate to see from equation (33) for unicycle kinematics. In addition, observe from (25) that all $\mathbf{d_i}$ being null implies that the unicycle agents are static, i.e., the stable equilibrium is a static configuration. □

Following the discussion above on local stability results for our system, let us now start the study of global convergence by presenting a Lemma that will be useful in the subsequent development.

Lemma 1. *Let m_1 and m_2 be two maximal cliques of $\mathcal{G}_f$ corresponding to two adjacent nodes in $\mathcal{C}_2(\mathcal{G}_f)$. Assume the following conditions are satisfied:*

L1) $\mathbf{d_i} = \mathbf{0}$, $i = 1, ..., N$.

L2) $card(I_{m_1} \bigcap I_{m_2}) = 2$, denote $I_{m_1} \bigcap I_{m_2} = \{i_1, i_2\}$.

L3) $C_i = \{m_1, m_2\}, i = i_1, i_2$.

L4) $\mathbf{d_{i_{m_1}}} = \mathbf{0}$, $\forall i \in I_{m_1}, i \neq i_1, i \neq i_2$.

Then, it holds that $\mathbf{d_{i_{m_1}}} = \mathbf{0}\, \forall i \in I_{m_1}$, $\mathbf{d_{i_{1_{m_2}}}} = \mathbf{d_{i_{2_{m_2}}}} = \mathbf{0}$, the rotation matrices in (7) satisfy $\mathbf{R_{m_1}} = \mathbf{R_{m_2}}$, and γ_{m_1} (4) is zero.

Proof. Let us choose, without loss of generality, the global reference frame for which $\mathbf{R_{m_1}} = \mathbf{I_2}$, i.e., $\alpha_{m_1} = 0$ (13). Considering L1 and L4, we can write, using (23):

$$\mathbf{d_i} = \mathbf{d_{i_{m_1}}} = \sum_{j \in I_{m_1}} \mathbf{q_{ji}} - \mathbf{c_{ji}} = \mathbf{0}, \forall i \in I_{m_1}, i \neq i_1, i \neq i_2. \quad (34)$$

Let us use that $\mathbf{q_{ji}} = -\mathbf{q_{ij}}$, $\mathbf{c_{ji}} = -\mathbf{c_{ij}}$ and interchange the names of the subscripts j and i in (34), to obtain:

$$\sum_{i \in I_{m_1}} \mathbf{q_{ji}} = \sum_{i \in I_{m_1}} \mathbf{c_{ji}}, \ \forall j \in I_{m_1}, j \neq i_1, j \neq i_2. \quad (35)$$

Imposing the condition $\alpha_{m_1} = 0$ in (13), we can write:

$$\sum_{j \in I_{m_1}} \mathbf{S^T_{qj,m_1}} \mathbf{S^{\perp}_{cj,m_1}} =$$
$$\sum_{\substack{j \in I_{m_1} \\ j \neq i_1, j \neq i_2}} \mathbf{S^T_{qj,m_1}} \mathbf{S^{\perp}_{cj,m_1}} + \sum_{j = i_1, i_2} \mathbf{S^T_{qj,m_1}} \mathbf{S^{\perp}_{cj,m_1}} = 0, \quad (36)$$

where the sums are for the clique m_1, i.e.,: $\mathbf{S_{qj,m_1}} = \sum_{i \in I_{m_1}} \mathbf{q_{ji}}$, $\mathbf{S_{cj,m_1}} = \sum_{i \in I_{m_1}} \mathbf{c_{ji}}$. Observe that, due to (35), $\mathbf{S_{qj,m_1}} = \mathbf{S_{cj,m_1}}\, \forall j \in I_{m_1}, j \neq i_1, j \neq i_2$. Thus, each of the addends in the first summation in the second line of (36) is a dot product of two orthogonal vectors, and therefore vanishes. Then, we have:

$$\sum_{j = i_1, i_2} \mathbf{S^T_{qj,m_1}} \mathbf{S^{\perp}_{cj,m_1}} = \mathbf{S^T_{qi_1,m_1}} \mathbf{S^{\perp}_{ci_1,m_1}} + \mathbf{S^T_{qi_2,m_1}} \mathbf{S^{\perp}_{ci_2,m_1}} =$$
$$\sum_{i \in I_{m_1}} \mathbf{q^T_{i_1 i}} \sum_{i \in I_{m_1}} \mathbf{c^{\perp}_{i_1 i}} + \sum_{i \in I_{m_1}} \mathbf{q^T_{i_2 i}} \sum_{i \in I_{m_1}} \mathbf{c^{\perp}_{i_2 i}} = 0. \quad (37)$$

Let us now focus on agents i_1 and i_2 and find constraints on their desired motion vectors which, along with the condition in (37), will lead to our result. From L3, these two agents belong to cliques m_1 and m_2 only and, due to L1, we have:

$$\mathbf{d_{i_1}} = \mathbf{d_{i_{1_{m_1}}}} + \mathbf{d_{i_{1_{m_2}}}} = \mathbf{0}$$
$$\mathbf{d_{i_2}} = \mathbf{d_{i_{2_{m_1}}}} + \mathbf{d_{i_{2_{m_2}}}} = \mathbf{0}. \quad (38)$$

Observe that the sum of partial desired vectors for any given clique is null, as can be directly seen by considering the expression for the partial vectors in (22), and using equation (19), as follows:

$$\sum_{i \in I_m} \mathbf{d_{i_m}} = \sum_{i \in I_m} \sum_{j \in I_m} \mathbf{q_{ji}} - \mathbf{R_m} \mathbf{c_{ji}} = \mathbf{0}, \ \ m = 1, ..., M. \quad (39)$$

Consider the above condition for clique $m = m_1$ in particular. Due to L4, its sum of vectors includes only agents i_1 and i_2. Thus:

$$\sum_{i \in I_{m_1}} \mathbf{d_{i_{m_1}}} = \mathbf{d_{i_{1_{m_1}}}} + \mathbf{d_{i_{2_{m_1}}}} = \mathbf{0}, \quad (40)$$

an expression which will be useful later on in the proof. Observe now, from (22), that:

$$\mathbf{d_{i_{m_1}}} = \sum_{j \in I_{m_1}} \mathbf{q_{ji}} - \mathbf{c_{ji}}, \ \ i = i_1, i_2. \quad (41)$$

$$\mathbf{d_{i_{m_2}}} = \sum_{j \in I_{m_2}} \mathbf{q_{ji}} - \mathbf{R_{m_2}} \mathbf{c_{ji}}, \ \ i = i_1, i_2. \quad (42)$$

Interchanging the subscripts i and j in (41), and then expressing the equations for $j = i_1$ and $j = i_2$ separately, we can write:

$$\sum_{i \in I_{m_1}} \mathbf{q_{i_1 i}} = -\mathbf{d_{i_{1_{m_1}}}} + \sum_{i \in I_{m_1}} \mathbf{c_{i_1 i}}$$
$$\sum_{i \in I_{m_1}} \mathbf{q_{i_2 i}} = -\mathbf{d_{i_{2_{m_1}}}} + \sum_{i \in I_{m_1}} \mathbf{c_{i_2 i}}. \quad (43)$$

Analogously, from (42), we obtain:

$$\sum_{i\in I_{m_2}} \mathbf{q_{i_1 i}} = -\mathbf{d_{i_{1m_2}}} + \mathbf{R_{m_2}} \sum_{i\in I_{m_2}} \mathbf{c_{i_1 i}}$$
$$\sum_{i\in I_{m_2}} \mathbf{q_{i_2 i}} = -\mathbf{d_{i_{2m_2}}} + \mathbf{R_{m_2}} \sum_{i\in I_{m_2}} \mathbf{c_{i_2 i}}. \quad (44)$$

Now, by substituting (43) in (37), we have:

$$\mathbf{d^T_{i_{1m_1}}} \sum_{i\in I_{m_1}} \mathbf{c^{\perp}_{i_1 i}} + \mathbf{d^T_{i_{2m_1}}} \sum_{i\in I_{m_1}} \mathbf{c^{\perp}_{i_2 i}} = 0, \quad (45)$$

and using in (45) that, from (40), $\mathbf{d_{i_{1m_1}}} = -\mathbf{d_{i_{2m_1}}}$, gives:

$$\mathbf{d^T_{i_{1m_1}}} (\sum_{i\in I_{m_1}} \mathbf{c^{\perp}_{i_1 i}} - \mathbf{c^{\perp}_{i_2 i}}) = \mathbf{d^T_{i_{1m_1}}} \mathbf{c^{\perp}_{i_1 i_2}} = \mathbf{d^T_{i_{2m_1}}} \mathbf{c^{\perp}_{i_1 i_2}} = 0. \quad (46)$$

Observe that (46) indicates that $\mathbf{d_{i_{1m_1}}}$ and $\mathbf{d_{i_{2m_1}}}$ are parallel to $\mathbf{c_{i_1 i_2}}$. We can then write:

$$\mathbf{d_{i_{1m_1}}} - \mathbf{d_{i_{2m_1}}} = k_{12}\mathbf{c_{i_1 i_2}}, \quad (47)$$

and, substituting (38) in (47):

$$\mathbf{d_{i_{1m_2}}} - \mathbf{d_{i_{2m_2}}} = -k_{12}\mathbf{c_{i_1 i_2}}, \quad (48)$$

for some scalar k_{12}. We now define $\mathbf{d'_{i_m}} = \mathbf{d_{i_m}}/N_m$, $i = i_1, i_2$, $m = m_1, m_2$. Notice that subtracting the two equations in (43), we have:

$$\mathbf{q_{i_1 i_2}} = -\mathbf{d'_{i_{1m_1}}} + \mathbf{d'_{i_{2m_1}}} + \mathbf{c_{i_1 i_2}}. \quad (49)$$

Then, substituting (47) yields:

$$\mathbf{q_{i_1 i_2}} = (1 - (k_{12}/N_{m_1}))\mathbf{c_{i_1 i_2}}. \quad (50)$$

On the other hand, subtraction of the equations in (44) gives:

$$\mathbf{q_{i_1 i_2}} = -\mathbf{d'_{i_{1m_2}}} + \mathbf{d'_{i_{2m_2}}} + \mathbf{R_{m_2}}\mathbf{c_{i_1 i_2}}, \quad i.e.,$$
$$\mathbf{q_{i_1 i_2}} + \mathbf{d'_{i_{1m_2}}} - \mathbf{d'_{i_{2m_2}}} = \mathbf{R_{m_2}}\mathbf{c_{i_1 i_2}}. \quad (51)$$

Substituting (48) and (50) in the left-hand side of (51) yields:

$$(1 - \kappa)\mathbf{c_{i_1 i_2}} = \mathbf{R_{m_2}}\mathbf{c_{i_1 i_2}}, \quad (52)$$

where $\kappa = k_{12}[(1/N_{m_1}) + (1/N_{m_2})]$. As multiplying by $\mathbf{R_{m_2}}$ does not modify the norm of $\mathbf{c_{i_1 i_2}}$, and disregarding the case $\kappa = 2$, that can be seen to correspond to a degenerate configuration in which $\mathbf{q_{i_1 i_2}} = \mathbf{c_{i_1 i_2}}(N_{m_1} - N_{m_2})/(N_{m_1} + N_{m_2})$, see (50), we clearly have that (52) can hold only if $k_{12} = 0$ and $\mathbf{R_{m_2}} = \mathbf{I_2} = \mathbf{R_{m_1}}$. Therefore, from (47), $\mathbf{d_{i_{1m_1}}} = \mathbf{d_{i_{2m_1}}}$. Then, due to (40), these two vectors are null. This implies $\mathbf{d_{i_{m_1}}} = \mathbf{0}\ \forall i \in I_{m_1}$ and hence, substituting (22) in (4), we see that $\gamma_{m_1} = 0$. Moreover, from (38), $\mathbf{d_{i_{1m_2}}} = \mathbf{d_{i_{2m_2}}} = \mathbf{0}$. □

In search of global convergence guarantees, we formulate the following assumptions regarding the formation graph:

A2) $card(I_m \bigcap I_n) = 2\ \forall \{m, n\} \in \mathcal{E}_{\mathcal{C}_2}$, $I_m \bigcap I_n = \emptyset$ otherwise *(i.e., every intersection set of two maximal cliques of $\mathcal{G}_f$ either contains exactly two agents, or is empty).*

A3) $I_m \bigcap I_n \bigcap I_r = \emptyset, m \neq n, m \neq r, n \neq r,\ m, n, r \in 1, .., M$ *(i.e., the intersection sets between maximal cliques of $\mathcal{G}_f$ are mutually disjoint).*

A4) $\mathcal{C}_2(\mathcal{G}_f)$ is a tree.

Note that we replace A1 by the stronger condition A4. Clearly, Theorem 1 and Corollary 1 hold if A4 does. We enunciate next our global stability result.

Theorem 2. *Suppose A2-A4 are satisfied. Then, the multiagent system under the control laws (24), for single-integrator kinematics, or (25), for unicycle kinematics, converges globally to the desired configuration, and the attained formation is static.*

Proof. We build on the development presented for Theorem 1, using the same Lyapunov candidate function $V = \gamma$. We proceed by examining the possible stable equilibriums of the system, and showing that they only include the case $V = 0$. From Corollary 1, a stable equilibrium is characterized, for the two kinematic models considered, by the condition $\mathbf{d_i} = \mathbf{0}$, $i = 1, ..., N$. Let us assume this condition is satisfied. Then, the rest of the proof relies on applying Lemma 1 to pairs of nodes in $\mathcal{C}_2(\mathcal{G}_f)$, i.e., pairs of maximal cliques in $\mathcal{G}_f$. Clearly, the assumption that all $\mathbf{d_i} = \mathbf{0}$, A2, and A3 together imply that conditions L1, L2 and L3 of Lemma 1 are always satisfied for any pair of adjacent nodes in $\mathcal{C}_2(\mathcal{G}_f)$. Thus, to see if Lemma 1 is applicable to a given couple of nodes, we will only need to check if L4 is satisfied. Consider then a given leaf node l in $\mathcal{C}_2(\mathcal{G}_f)$, which is a tree (A4), and its adjacent node a. Denote $I_l \bigcap I_a = \{r_1, r_2\}$. Being a leaf node, and due to A2, all the agents in l except r_1 and r_2 belong to maximal clique l only, and thus their partial desired vectors satisfy, from (23), $\mathbf{d_{i_l}} = \mathbf{d_i} = \mathbf{0}, i \in I_l, i \neq r_1, i \neq r_2$. Then, clearly, L4 holds and Lemma 1 can be applied to the pair l (in the role of m_1) and a (in the role of m_2). This way, by extension, it is ensured that for every clique m that is a leaf node of $\mathcal{C}_2(\mathcal{G}_f)$, $\gamma_m = 0$ and $\mathbf{d_{i_m}} = \mathbf{0}\ \forall i \in I_m$.

Let us define $\mathcal{C}^r_2(\mathcal{G}_f)$ as the induced subgraph of $\mathcal{C}_2(\mathcal{G}_f)$ containing all its nodes except the leaves. Clearly, $\mathcal{C}^r_2(\mathcal{G}_f)$ is also a tree. Let us consider any one of its leaf nodes, and denote it as l^r. We have:

1) For every agent i belonging only to l^r, (i.e., $C_i = \{l^r\}$), from (23), $\mathbf{d_{i_{l^r}}} = \mathbf{d_i} = \mathbf{0}$.

2) Notice l^r is adjacent to one or multiple leaves of $\mathcal{C}_2(\mathcal{G}_f)$. As we just showed, all the partial desired motion vectors corresponding to leaf nodes of $\mathcal{C}_2(\mathcal{G}_f)$ are null. Then, for the agents i shared by l^r and a leaf of $\mathcal{C}_2(\mathcal{G}_f)$, $\mathbf{d_i} = \mathbf{d_{i_{l^r}}}$. Since all $\mathbf{d_i}$ are assumed null, we have $\mathbf{d_{i_{l^r}}} = \mathbf{0}$.

3) Being a leaf node of $\mathcal{C}^r_2(\mathcal{G}_f)$, l^r is adjacent to exactly one node, which we denote as a^r, that is not a leaf node of $\mathcal{C}_2(\mathcal{G}_f)$. These two maximal cliques share two agents; let us denote $I_{l^r} \bigcap I_{a^r} = \{r^r_1, r^r_2\}$.

As, clearly, points 1), 2) and 3) encompass all the agents in clique l^r, we have $\mathbf{d_{i_{l^r}}} = \mathbf{0}\ \forall i \in I_{l^r}, i \neq r^r_1, i \neq r^r_2$. Thus, we can apply Lemma 1 to l^r (in the role of m_1) and a^r (in the role of m_2), since L4 holds for this pair of cliques. In consequence, for every node m that is a leaf of $\mathcal{C}^r_2(\mathcal{G}_f)$, $\gamma_m = 0$ and $\mathbf{d_{i_m}} = \mathbf{0}\ \forall i \in I_m$, i.e., the same result shown above for the leaves of $\mathcal{C}_2(\mathcal{G}_f)$.

It is then clear that we can consider subsequent induced tree subgraphs of $\mathcal{C}^r_2(\mathcal{G}_f)$ and apply the reasoning above recursively, until reaching a trivial case (a final, irreducible tree with either one or two nodes). As a result, we have that $\gamma_m = 0$ for all the nodes in $\mathcal{C}_2(\mathcal{G}_f)$, i.e., for all the M maximal cliques. We can conclude, then, that if $\mathbf{d_i} = \mathbf{0}, \ i = 1, ..., N$, i.e., if $\dot{V} = 0$ for all time (Corollary 1), it holds that $\gamma_m = 0, \ m = 1, ..., M$, i.e., $V = 0$. The converse is also true since $V = \gamma = 0$, see (4), (6), implies $\mathbf{d_i} = \mathbf{0}, \ i = 1, ..., N$ (23). Hence, $\dot{V} = 0$ for all time $\Leftrightarrow V = 0$, i.e., the multiagent system converges globally to the desired formation. In addition, from Corollary 1, the configuration the agents reach is static. □

V. Discussion of valid formation graph topologies

We analyze in this section the characteristics of $\mathcal{G}_f$ arising from the introduced topological assumptions. Let us start by considering A1. A formation graph satisfying this assumption is illustrated in Fig. 3. Firstly, we note that A1 specifies a class of graphs that are rigid in two dimensions. To see this, observe first that a clique is a rigid graph. Assume the intersection of every pair of maximal cliques of $\mathcal{G}_f$ corresponding to adjacent nodes of $\mathcal{C}_2(\mathcal{G}_f)$ contains exactly two nodes. Notice then that, due to A1, $\mathcal{G}_f$ can be constructed, starting from one of its maximal cliques, by applying successive edge-attachment operations, as defined in [17], to incorporate all the other maximal cliques. These operations consist in merging an edge of each of two given graphs into a single edge of a new graph that is a fusion of the two. In [17], it was shown that such edge-attachment procedures generate a rigid graph for two input graphs that are rigid. Thus, clearly, $\mathcal{G}_f$ is rigid in two dimensions. If there are adjacent nodes in $\mathcal{C}_2(\mathcal{G}_f)$ associated with maximal cliques of $\mathcal{G}_f$ which share more than two nodes, one can always eliminate some of the edges to obtain a subgraph of $\mathcal{G}_f$ for which the relevant maximal clique intersections are two-node, and thus the reasoning above also applies. Note that not all rigid graphs satisfy A1.

As shown in the previous section, global convergence to the desired formation is guaranteed for any formation graph whose topology conforms with A2-A4. Clearly, this augmented set of assumptions also implies the graph is rigid in two dimensions. The class of rigid graphs satisfying A2-A4 is illustrated with four exemplary topologies, containing maximal cliques of up to six agents, in Fig. 4. Observe that the specification resulting from these assumptions provides flexibility, as it allows structures that are made up from maximal cliques of different sizes, and can be extended to arbitrary numbers of nodes. For instance, the chained structure in bottom-left of the figure can be prolonged to contain any number of four-node maximal cliques, and a more general topology with heterogeneous maximal cliques, such as the example depicted in the center, is also arbitrarily extendable. Observe that, regardless of the total number of nodes in $\mathcal{G}_f$, any given agent only has to interact with (i.e., measure the relative position of) a small number of neighbors, which indicates the distributed and partial information-based nature of our controller. We require a denser (i.e., with more edges) formation graph than distance-based formation controllers, which are valid for general rigid graphs, but let us note that as the number of agents grows, the minimum number of edges we need is in the same order as the number of edges in a minimally rigid graph.

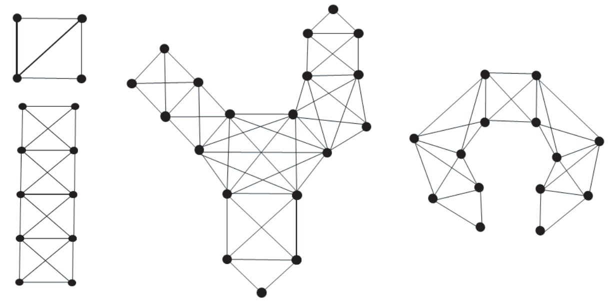

Fig. 4. Four examples of formation graph topologies satisfying assumptions A2-A4, i.e., for which the proposed controller is provably globally stable.

VI. Simulations

In this section, the effectiveness of our controller is illustrated in simulation. In our tests, we considered that a sensing or communication infrastructure in the team of agents allowed each of them to measure the relative positions of its neighbors in $\mathcal{G}_f$, as commented in Section II. We first present results from an example where the desired formation was composed of twelve unicycle agents arranged in two concentric circles. The formation graph $\mathcal{G}_f$ consisted of five maximal cliques, each containing four agents, with the chained structure depicted in bottom-left of Fig. 4. Figure 5 displays the paths followed by the agents using our proposed controller, showing how they reach the formation from an arbitrary initial configuration. The control law was computed for each agent in a local reference frame aligned with its heading. Observe that the final group shape has arbitrary translation and rotation in the workspace. Notice as well that the final headings of the agents are arbitrary. It would be straightforward to control these headings, if desired, by making the agents rotate in place once the formation has been attained. We also display in the same figure the linear and angular velocities of the agents and the evolution of the angles, expressed in a common reference frame, of the rotation matrices $\mathbf{R_m}$ for the five maximal cliques. It can be observed that the angles converge to a common value as the formation is achieved. The vanishing global and partial cost functions are also depicted.

We also illustrate a second example where a group of forty agents was considered. This time, the agents obeyed the single-integrator kinematic model. The simulation results for this example are displayed in Fig. 6. The geometry of the rigid desired formation and the edges of the formation graph $\mathcal{G}_f$, which consisted of eighteen maximal cliques of sizes ranging from three to six agents, are shown. Notice that this graph also belongs to the class defined by assumptions A2-A4, for which our controller guarantees global formation stabilization. Since single-integrator agents do not have a defined heading, we computed the control law considering for each agent an arbitrarily oriented local reference frame. The paths followed by the agents when using our proposed controller illustrate their successful convergence to a pattern having the same shape and size as the desired one. We also display the norms of the instantaneous velocity vectors $\mathbf{u_i}$, the cost functions, and the angles of the rotation matrices for each of the maximal cliques. These angles, expressed in a common reference frame,

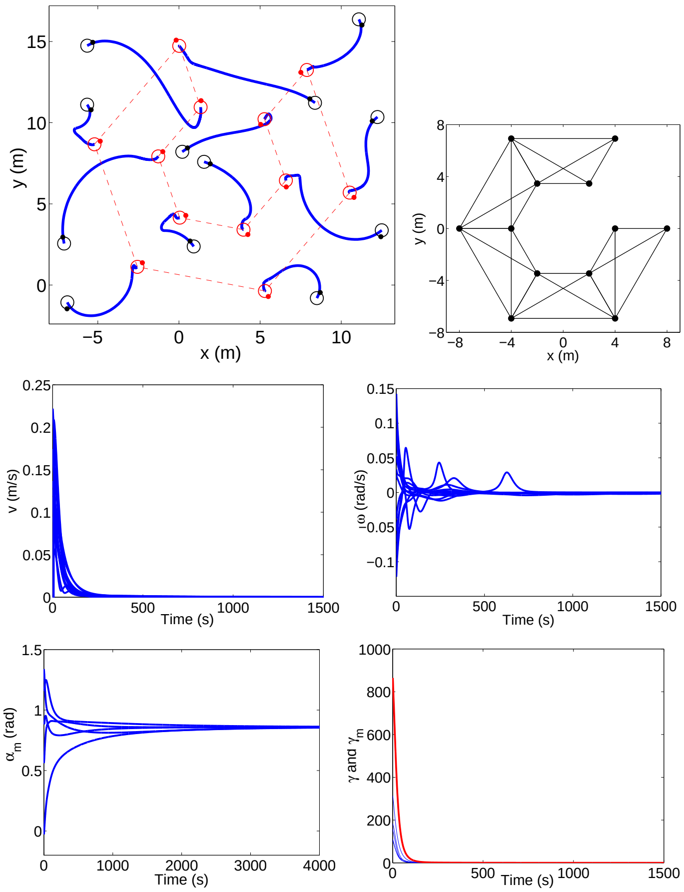

Fig. 5. Simulation results for the twelve-agent example. Top row: Paths followed by the agents; the final positions are shown joined by dashed lines (left). Desired geometric configuration; adjacent agents in the formation graph are joined by lines (right). Middle row: Evolution of the linear (left) and angular (right) velocities of the agents. Bottom row: Evolution of the rotation matrix angles for the maximal cliques (left). Evolution of the maximal-clique cost functions γ_m and the global γ, which is plotted in a thicker line (right).

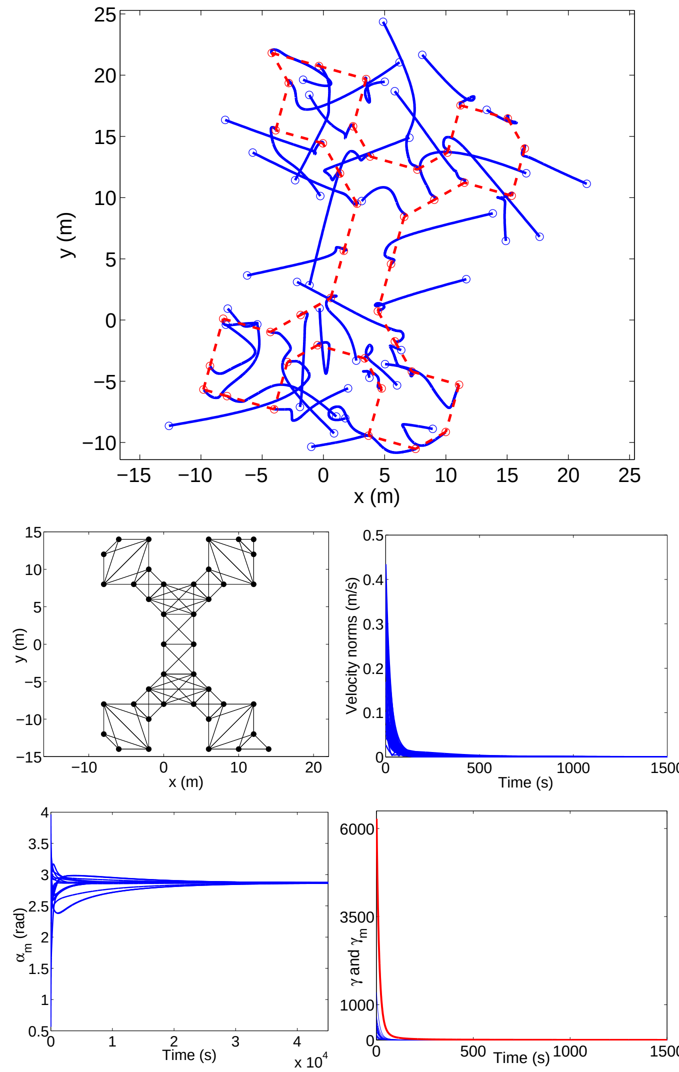

Fig. 6. Simulation results for the forty-agent example. Top row: Paths followed by the agents. The final positions are shown joined by dashed lines. Middle row: Desired geometric configuration; adjacent agents in the formation graph are joined by lines (left). Evolution of the norms of the agents' velocity vectors (right). Bottom row: Evolution of the rotation matrix angles for the maximal cliques (left). Evolution of the maximal-clique cost functions γ_m and the global γ, which is plotted in a thicker line (right).

converge to a common value as the rigid desired formation is attained.

VII. Conclusion

We have presented a distributed control method to stabilize a set of mobile agents to a rigid formation. To alleviate the need for the agents to rely on centralized sensing or shared reference systems, we have proposed a coordinate-free approach which can be implemented using only partial relative position information measured locally. Our controller can be used on unicycle-type platforms and has been shown to be globally stable for a class of rigid formation graphs. Possible directions for future work include addressing a similar distributed stabilization problem in 3D space, where rigidity-related graph conditions are in general more complex to characterize. In addition, it can be interesting to study the case where the formation graph is considered to change dynamically as the agents move.

Acknowledgment

The authors wish to thank María L. Rodríguez-Arévalo for helpful discussions regarding graph theory.

References

[1] M. Mesbahi and M. Egerstedt, *Graph theoretic methods in multiagent networks*. Princeton University Press, 2010.

[2] M. M. Zavlanos and G. J. Pappas, "Distributed formation control with permutation symmetries," in *IEEE Conference on Decision and Control*, 2007, pp. 2894–2899.

[3] W. Dong and J. Farrell, "Cooperative control of multiple nonholonomic mobile agents," *IEEE Transactions on Automatic Control*, vol. 53 (6), pp. 1434–1448, 2008.

[4] L. Sabattini, C. Secchi, and C. Fantuzzi, "Arbitrarily shaped formations of mobile robots: artificial potential fields and coordinate transformation," *Autonomous Robots*, vol. 30 (4), pp. 385–397, 2011.

[5] J. Alonso-Mora, A. Breitenmoser, M. Rufli, R. Siegwart, and P. Beardsley, "Image and animation display with multiple mobile robots," *Int. J. Rob. Res.*, vol. 31 (6), pp. 753–773, 2012.

[6] A. Becker, C. Onyuksel, T. Bretl, and J. McLurkin, "Controlling many differential-drive robots with uniform control inputs," *The International Journal of Robotics Research*, vol. 33 (13), pp. 1626–1644, 2014.

[7] Z. Lin, B. Francis, and M. Maggiore, "Necessary and sufficient graphical conditions for formation control of unicycles," *IEEE Transactions on Automatic Control*, vol. 50 (1), pp. 121–127, 2005.

[8] M. Ji and M. Egerstedt, "Distributed coordination control of multiagent systems while preserving connectedness," *IEEE Transactions on Robotics*, vol. 23 (4), pp. 693–703, 2007.
[9] D. V. Dimarogonas and K. J. Kyriakopoulos, "A connection between formation infeasibility and velocity alignment in kinematic multi-agent systems," *Automatica*, vol. 44 (10), pp. 2648–2654, 2008.
[10] J. Cortés, "Global and robust formation-shape stabilization of relative sensing networks," *Automatica*, vol. 45 (12), pp. 2754 – 2762, 2009.
[11] Z. Kan, A. Dani, J. Shea, and W. Dixon, "Network connectivity preserving formation stabilization and obstacle avoidance via a decentralized controller," *IEEE Transactions on Automatic Control*, vol. 57 (7), pp. 1827–1832, 2012.
[12] H. G. Tanner and A. Boddu, "Multiagent navigation functions revisited," *IEEE Transactions on Robotics*, vol. 28 (6), pp. 1346–1359, 2012.
[13] K.-K. Oh and H.-S. Ahn, "Formation control and network localization via orientation alignment," *IEEE Transactions on Automatic Control*, vol. 59 (2), pp. 540–545, 2014.
[14] M. Franceschelli and A. Gasparri, "Gossip-based centroid and common reference frame estimation in multiagent systems," *IEEE Transactions on Robotics*, vol. 30 (2), pp. 524–531, 2014.
[15] K.-K. Oh, M.-C. Park, and H.-S. Ahn, "A survey of multi-agent formation control," *Automatica*, vol. 53, pp. 424–440, 2015.
[16] E. Montijano, D. Zhou, M. Schwager, and C. Sagüés, "Distributed formation control without a global reference frame," in *American Control Conference*, 2014, pp. 3862–3867.
[17] R. Olfati-Saber and R. M. Murray, "Graph rigidity and distributed formation stabilization of multi-vehicle systems," in *Proceedings of the IEEE Int. Conference on Decision and Control*, 2002, pp. 2965–2971.
[18] D. V. Dimarogonas and K. H. Johansson, "Further results on the stability of distance-based multi-robot formations," in *American Control Conference*, 2009, pp. 2972–2977.
[19] L. Krick, M. E. Broucke, and B. A. Francis, "Stabilisation of infinitesimally rigid formations of multi-robot networks," *International Journal of Control*, vol. 82 (3), pp. 423–439, 2009.
[20] J. Guo, Z. Lin, M. Cao, and G. Yan, "Adaptive control schemes for mobile robot formations with triangularised structures," *IET Control Theory and Applications*, vol. 4 (9), pp. 1817–1827, 2010.
[21] K.-K. Oh and H.-S. Ahn, "Formation control of mobile agents based on inter-agent distance dynamics," *Automatica*, vol. 47 (10), pp. 2306 – 2312, 2011.
[22] H. García de Marina, M. Cao, and B. Jayawardhana, "Controlling rigid formations of mobile agents under inconsistent measurements," *IEEE Transactions on Robotics*, vol. 31 (1), pp. 31–39, 2015.
[23] B. D. O. Anderson, C. Yu, B. Fidan, and J. M. Hendrickx, "Rigid graph control architectures for autonomous formations," *IEEE Control Systems*, vol. 28 (6), pp. 48–63, 2008.
[24] B. D. O. Anderson, "Morse theory and formation control," in *Mediterranean Conference on Control Automation*, 2011, pp. 656–661.
[25] Z. Lin, L. Wang, Z. Han, and M. Fu, "Distributed formation control of multi-agent systems using complex Laplacian," *IEEE Transactions on Automatic Control*, vol. 59 (7), pp. 1765–1777, 2014.
[26] Y.-P. Tian and Q. Wang, "Global stabilization of rigid formations in the plane," *Automatica*, vol. 49 (5), pp. 1436–1441, 2013.
[27] J. Desai, J. Ostrowski, and V. Kumar, "Modeling and control of formations of nonholonomic mobile robots," *IEEE Transactions on Robotics and Automation*, vol. 17 (6), pp. 905–908, 2001.
[28] N. Moshtagh, N. Michael, A. Jadbabaie, and K. Daniilidis, "Vision-based, distributed control laws for motion coordination of nonholonomic robots," *IEEE Trans. Robotics*, vol. 25 (4), pp. 851–860, 2009.
[29] G. López-Nicolás, M. Aranda, Y. Mezouar, and C. Sagüés, "Visual control for multirobot organized rendezvous," *IEEE Trans. Sys., Man, and Cybern., Part B: Cybern.*, vol. 42 (4), pp. 1155–1168, 2012.
[30] M. Aranda, G. López-Nicolás, C. Sagüés, and Y. Mezouar, "Formation control of mobile robots using multiple aerial cameras," *IEEE Transactions on Robotics*, vol. 31 (4), pp. 1064–1071, 2015.
[31] N. Michael, J. Fink, and V. Kumar, "Controlling ensembles of robots via a supervisory aerial robot," *Advanced Robotics*, vol. 22 (12), pp. 1361–1377, 2008.
[32] M. Aranda, G. López-Nicolás, C. Sagüés, and M. M. Zavlanos, "Three-dimensional multirobot formation control for target enclosing," in *IEEE/RSJ Int. Conf. on Intell. Robots and Systems*, 2014, pp. 357–362.
[33] ——, "Coordinate-free formation stabilization based on relative position measurements," *Automatica*, vol. 57, pp. 11–20, 2015.
[34] T. A. McKee and F. R. McMorris, *Topics in intersection graph theory*. Society for Industr. and Applied Math. (SIAM), Philadelphia, PA, 1999.
[35] J. C. Gower and G. B. Dijksterhuis, *Procrustes problems*. Oxford University Press, 2004.